Image Anal Stereol 2025;44:39-47 doi: 105566/ias.3143
Original Research Paper

RESEARCH ON VISUAL DETECTION METHOD OF SOUND FILM BROKEN GLUE DEFECT

JIANCHUN LIU✉ [1,2], XUNJIN JIANG[1], CHAOQI HUANG[1] AND YUQUAN LIN[3]

[1]School of Mechanical and Automotive Engineering, Xiamen University of Technology, Xiamen 361024, China, [2]Xiamen Key Laboratory of Robot System and Digital Manufacturing, Xiamen, 361024, China, [3]Xiamen East Sound Electronics Co., LTD., Xiamen, 361101, China
e-mail: xmutljc@163.com; jiangxunjin2163.com; huang_chaoqi@foxmail.com; linyuquan520@163.com
(Received January 26, 2024; revised December 2, 2024; accepted December 16, 2024)

ABSTRACT

Broken glue defect is a common defect in sound film dispensing. Aiming at the problem of fuzzy glue region boundary frequently occurring in the detection process, an improved iterative maximum interclass variance method was proposed to detect broken glue defects. Due to the skewness distribution of the gray curve of the sound film, the median value of the gray value of the image was replaced by the average value of the improved iterative method to eliminate the sound film. The initial threshold of the sound film dispensing region was quickly converged. The maximum inter-class variance method was combined to improve the extraction accuracy of the glue region boundary. The image features of single gap, multi gap, and dislocation defect types in qualified and broken products were compared, and the number and offset of glue areas were calculated to identify defects accurately. Fifteen thousand products were randomly selected on the production line for testing, and the results showed that the detection accuracy rate of qualified products was 100%, and the detection accuracy rate of broken glue was 99.1%, which met the needs of enterprises.

Keywords: Broken glue defect, Improved iteration, Maximum interclass variance method, Threshold segmentation.

INTRODUCTION

The sound film and the voice coil are the main vocal components of the micro loudspeaker, most of which are dispensed with the sound film by the dispensing machine, but the passing rate and accuracy of the dispensing are low, which affects the quality of the micro loudspeaker.

According to the characteristics of glue, machine vision is mainly used to detect the quality of glue. The glue area image taken is segmented by threshold value to obtain glue information and determine whether there are defects. Liao (2015) expressed the deviation of the glue line position by comparing the deviation between the feature points of the standard glue picture and the control points of the actual glue picture. He *et al*. (2020) obtained the target region using the traditional threshold segmentation method and then obtained the region outline of the subpixel edge fixer. The above methods must be manually thresholded and overly dependent on human experience. Zhang *et al*. (2021) used an improved Canny algorithm and maximum inter-class variance (OTSU) method to obtain the glue-coated area and then detected the defects with subtraction in the glue area of the standard picture. Chen *et al*. (2020) proposed a visual detection method for adhesive coating that did not rely on standard images. The standard adhesive coating trajectory was generated using engineering drawings, and the sampling points on the standard adhesive coating trajectory were converted into actual points through camera calibration to obtain adhesive strip information. Yu *et al*. (2023) proposed a method to detect the offset and width of gluing by K-Nearest Neighbor (KNN) classification without standard gluing pictures. Both methods measured linear gluing trajectories, but the accuracy of arc gluing trajectories was not well.

MATERIALS AND METHODS

DETECTION SYSTEM DESIGN

Hardware Design

A specific model of the sound film in the production line of the enterprise was taken as the detection object, as shown in Fig.1(a). The size of the sound film was $15\times11mm^2$, Z_1-frame 、 Z_2-frame surrounded the dispensing area, and the shape of the area was similar to a circular rounded rectangle. In production, detecting

whether the glue was broken in the dispensing area was necessary.

The detection scheme's hardware composition was shown in Fig.1(b), mainly composed of an industrial camera, lens, light source, etc. The detection workpiece was placed at the center of the platform. Above it, the industrial camera, lens, and light source were successively installed, and the focal length and working distance of the lens were meticulously adjusted until the camera captured a clear image. To ensure that the image could retain all product information, the camera field of view was 16×13mm^2, and the accuracy requirement was 0.02mm. Therefore, the pixel width in the long side direction was 800 pixels, and the pixel width in the short side direction was 650 pixels. Considering the distortion of the camera edge field of view and the stability requirements of the system, it was usually multiplied by 3 in industrial detection, that is, 2400×1950 pixels. Thus, selecting a camera with a resolution of 500W pixels could meet the requirements. The formula for calculating the focal length of an industrial lens was as follows:

$$f = Dw/(1 + 1/F) \quad (1)$$

Where f represented the lens's focal length, Dw represented the working distance, and F represented the magnification. The formula for calculating the focal length of an industrial lens was derived from the relationship between the lens, the working distance, and the magnification, and it was used to determine the appropriate lens for a given setup.

$$F = min\{h/H, v/V\} \quad (2)$$

Where h and v represented the length and width of the selected camera chip, and H and V represented the shooting field's length and width, respectively.

Given that the working distance Dw was 115mm, h was 12.4mm, and v was 9.8mm when formula (2) was substituted into formula (1), f was 49.4mm. A lens with a focal length of 50mm was selected. Since the color of the glue was similar to the background color of the dispensing area, both were red. The background was silver-white. Selecting a blue light source with a wavelength between 400 and 480nm eliminated the background color and significantly enhanced the glue area's contrast, providing a favorable environment for subsequent image processing.

Dispensing Defect

Under normal circumstances, the qualified glue was evenly distributed in the specified area, showing a whole attitude, the glue outline was clear, with no fracture, as shown in Fig.2(a). However, the occasional dispensing defects mainly included scraping, overflowing, and breaking glue. The first two defects can be identified directly by calculating the area of the glue. The glue-breaking defects can be divided into the following three situations:

1. A single gap in the glue track resulted in the glue head and tail not being connected, as shown in Fig.2(b).
2. There were multiple gaps in the glued track, and the guide glue was divided into multiple segments, as shown in Fig.2(c).
3. Glue hitting outside the specified area led to misalignment, as shown in Fig.2(d).

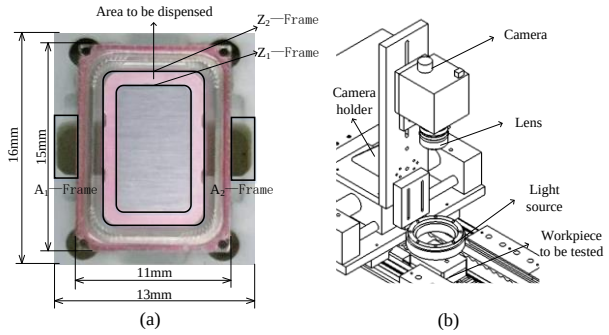

Fig. 1. *Sound film and detection apparatus: (a) Sound film image, (b) Testing mechanism diagram*

Among them, the first two defects were mainly caused by the glue nozzle's blockage, and the misplacement of the front cover caused the last one. Accurately identifying the type of broken glue defect can help enterprises quickly find the root cause of the problem and feed it back to the control system for rapid processing.

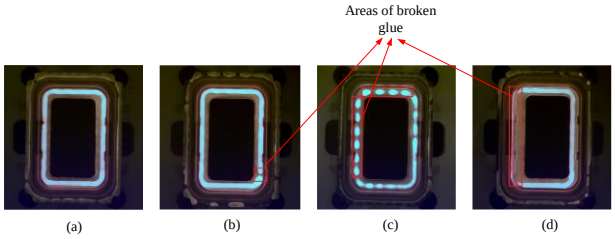

Fig.2. *Sound film dispensing image: (a) Qualified product, (b) Single gap, (c) Multiple gaps, (d) Misalignment*

SOUND FILM BROKEN GLUE DETECTION

Image Denoising

Since there was inevitable noise in the image, it affected the detection accuracy, so reducing the noise

processing was necessary. Standard methods for noise reduction with median filtering, mean filtering, and Gauss filtering(Liang *et al*., 2023), the experiment showed that the median filtering could effectively save the glue edge information, and the effect was better, as shown in Fig.3.

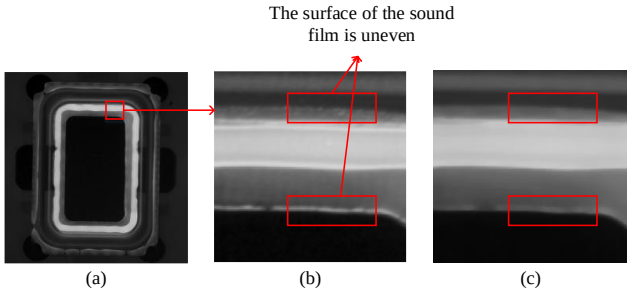

Fig.3. *Image filtering: (a) Pre-filtered image, (b) Noise area, (c) Filtered image*

Improved Iterative Maximum Inter-class Variance Method

The core of glue quality detection was threshold segmentation. OTSU method (Yu *et al*., 2022), as a classical threshold segmentation method, divided the image into background region and target region, and the segmentation effect was shown in Fig. 6(b). It can be found that when the traditional OTSU method divided the sound film dispensing image, the glue region could not be accurately extracted, resulting in poor anti-interference and insufficient stability. It was because the OTSU method had an excellent segmentation effect on images with bimodal gray distribution. However, when the image distribution was skewed, or there were abnormal data, the segmentation effect was not ideal. As shown in Fig.4 (a), the gray level curve of the sound film dispensing image belonged to the right-skewed distribution, the effect of directly using the OTSU method was not good, so abnormal data should be eliminated first. In order to make up for the shortcomings of the traditional OTSU method, the improved iterative method and OTSU method were combined to avoid the interference of abnormal data.

The iterative method was a global threshold segmentation method, which took the average gray value of the image as the starting point of segmentation, iterated continuously, and took the final convergence value as the final segmentation threshold (Li *et al*., 2022). The processing effect was shown in Fig.6(c), but the segmentation effect cannot meet the requirements. The main reason was that this method was mainly suitable for occasions where there was little difference between the target area and the background area. However, the target area of the research object was quite different from the background area. It can be seen from Fig.4(a) that the gray level distribution of the background area of the image belonged to the skewed distribution. For the data with skewed distribution, the median is not affected by the extreme value, which can better reflect the central tendency of the data. Therefore, GV_{m0}, the median gray value of the image, was selected as the primary threshold. After the initial segmentation, the sound film dispensing image was divided into the background area Z_g and the target area Z_t, the median gray value GV_{gm} in the Z_g area and the average gray value GV_{tm} in the Z_t area were calculated. The average GV_{mi} of GV_{gm} and GV_{tm} were continuously updated through iterative calculation until the difference between GV_m and GV_{mi} was less than Δt. The calculation process of the improved iterative method is shown in Fig.5. And the iterative calculation formula is shown in equation (3).

$$\begin{cases} GV_{mi} = \frac{GV_{gmi}+GV_{tmi}}{2} \\ |GV_m - GV_{mi}| < \triangle t \end{cases} \quad (3)$$

Finally, the threshold GV_m was used for image segmentation, and the gray level curve of the sound film after iteration was shown in Fig.4(b).

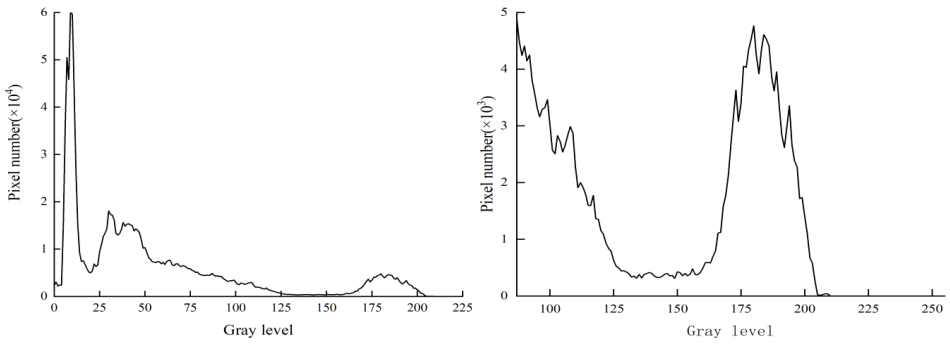

Fig.4. *Grayscale curve of sound film: (a) Pre-iteration, (b) After iteration*

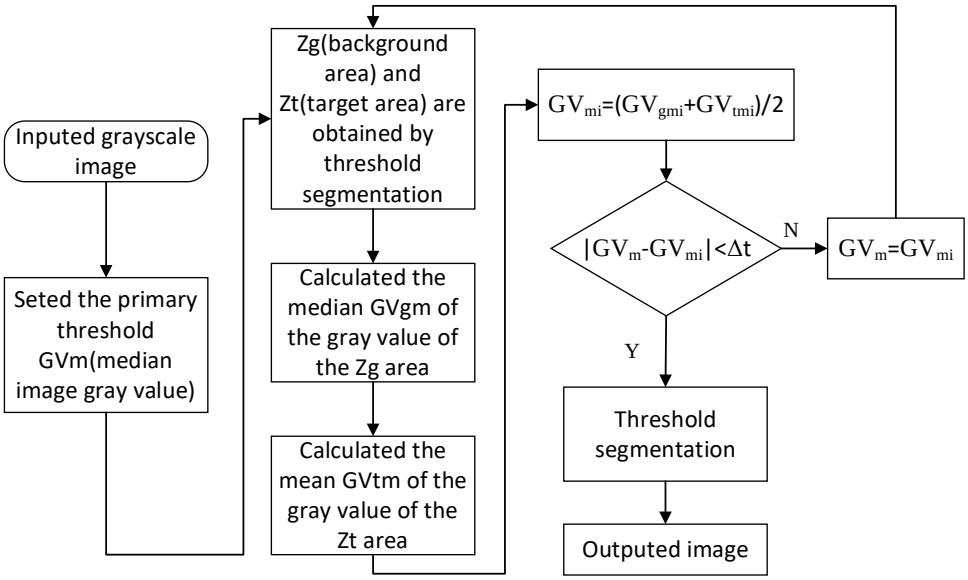

Fig.5. *Calculation flow of improved iterative method*

OTSU method mainly divided the gray image into two parts, the target C_1 and the background C_2, according to the threshold GV determined by the gray histogram, so the interclass variance of C_1 and C_2 was the largest(Guo *et al.*,2023).

$$\sigma^2 = p_1(GV_{m_1} - GV_M)^2 + p_2(GV_{m_2} - GV_M)^2 \quad (4)$$

σ^2 represented the interclass variance of C_1 and C_2, p_1 was the probability of the pixel in the C_1 area, p_2 was the probability of the pixel in the C_2 area, GV_{m1} was the average value of the gray value in the C_1 area, GV_{m2} was the average value of the gray value in the C_2 area, and GV_M was the average value of the total gray value of the image.

Assuming that the image gray level was L, then in the image of [0,1,2,3... L-1], the optimal threshold selection principle of OTSU method was as follows:

$$GV_b = \max\left(\sum_{i=0}^{L-1}\sigma^2\right) \quad (5)$$

When selecting the optimal threshold, OTSU method needed to traverse 0-255 gray levels for 8-bit images, which led to a lengthy calculation process. When Fig.6(a) was used as the input image, GV_m was used as the traversal starting point, and the maximum image gray value GV_{max} was used as the traversal endpoint, which reduced the traversal range. The improved method's processing effect was shown as Fig.6 (d).

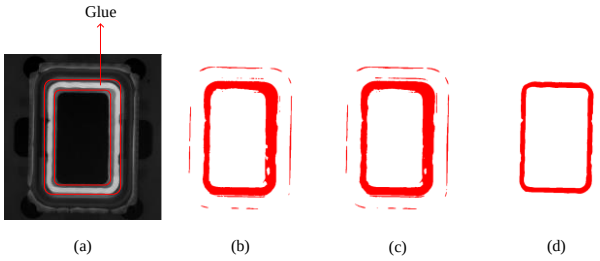

Fig. 6. *Comparison of segmentation effect: (a) Soundfilm dispensing image, (b) Traditional OTSU method, (c) Traditional iterative method, (d) Improved iterative maximum inter-class variance method*

The mean intersection over union (*MIOU*) was introduced as an image segmentation accuracy evaluation index to compare each algorithm's advantages and disadvantages in a quantitative analysis (Huang *et al.*, 2020). The larger the *MIOU* value, the better the image segmentation effect. *MIOU* was calculated as follows.

$$MIOU = \frac{1}{k+1} \bullet \frac{A \cap B}{A \cup B} \quad (6)$$

k represented the number of categories of the foreground target, A represented the number of pixels in the dispensing area, and B represented the number of pixels obtained by the segmentation of various algorithms. The average crossover ratio of different algorithms was calculated, as shown in Table 1.

Table1. *Comparison of segmentation effect of different algorithms*

Detection object	Evaluation index	Traditional OTSU	Iterative method	Textual algorithm
Sound film dispensing	Threshold value	87	85	141
	MIOU	0.273	0.257	0.497

As shown in Table 1, the proposed algorithm was superior to the iterative method and the traditional OTSU method in image segmentation accuracy, and the glue region obtained by segmentation had clear boundaries, better stability, and anti-interference.

SOUND FILM BROKEN GLUE RECOGNITION

The identification of sound film broken glue mainly includes edge location and glue detection. Edge location was to obtain the edge of the sound film and determine the product's position through coarse and fine positioning, then cut the image according to the edge to reduce the detection range. Glue detection first eliminated noise points through image denoising, then obtained the optimal threshold GV_b according to Improved iteration maximum interclass variance (IIMIV), and then got the glue region by threshold segmentation. The different regional characteristics were used to determine the types of broken glue defects. The specific detection process was shown in Fig.7.

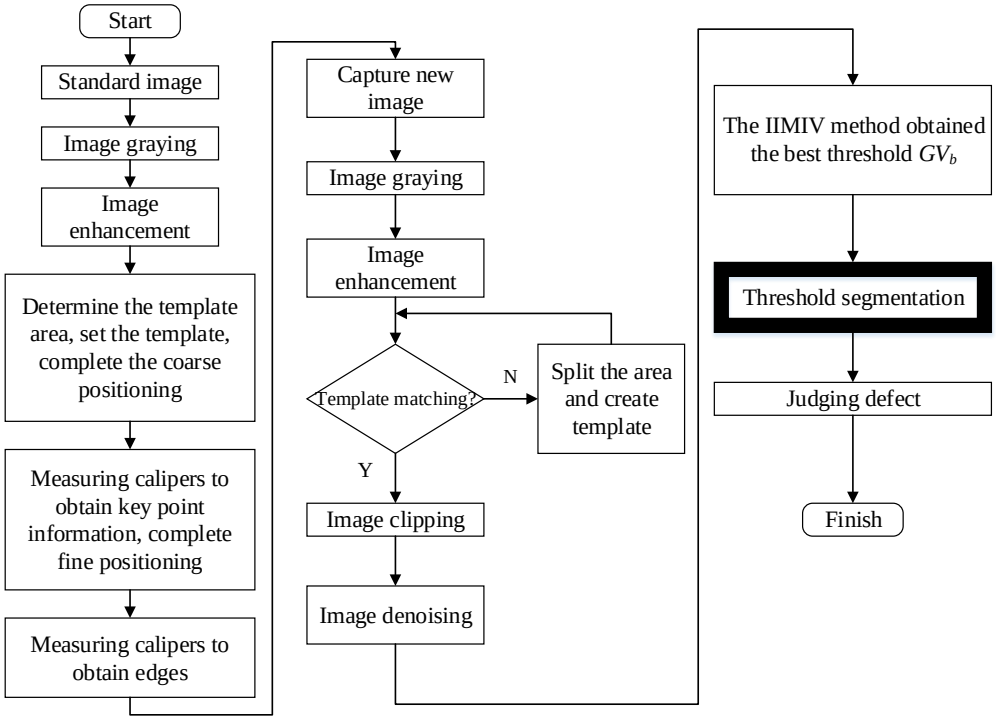

Fig. 7. *Glue testing process*

Template Matching

Due to the many complex factors affecting the dispensing quality, the track and shape of the glue on different sound films were slightly different, so it was not appropriate to choose the glue area directly as the template. In order to improve the accuracy of template matching, template selection must meet two conditions: ①The template area must be independent of the glue detection area. ② The position of the template area in the image was relatively fixed and easy to find. Therefore, A_1-Frame and A_2-Frame, as shown in Fig.1, were selected as templates.

After gray-scaling the image, the sound film base and edge contour were very fuzzy in the image, as shown in Fig.8(a), which could have been more conducive to template matching and positioning. The image needed to be enhanced, and linear gray transformation was used to change the gray value of each pixel in the image (Guo *et al*., 2022). The enhanced image was shown in Fig.8(b) and used as the template image.

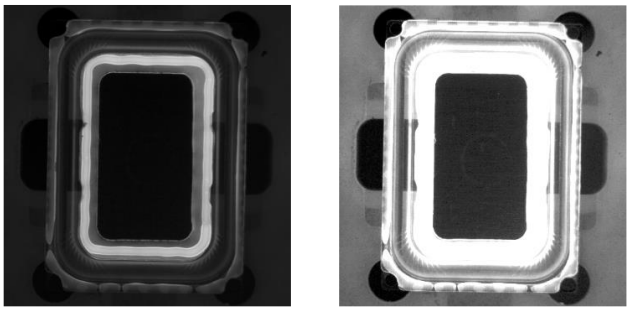

(a) (b)

Fig. 8. *Image enhancement: (a) Grayscale image, (b)Enhanced image*

Template matching methods included correlation-based template matching (Ma *et al*., 2019) and shape-based template matching(Shen et al., 2023). The two methods were used to compare and match 30 products, respectively, and the matching results were shown in Fig.9. As can be seen from Fig.9, the stability and matching scores of template matching based on correlation were better than those based on shape.

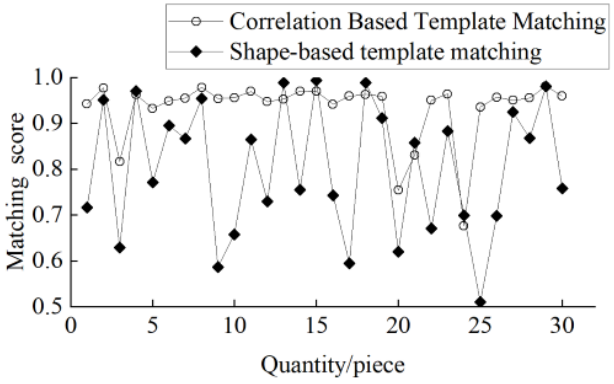

Fig. 9. *Comparison of template matching scores*

Product Positioning

After successfully creating the template, affine transformation was used to determine the product position (Zou et al., 2024). Due to the unclear contrast between the edge of the sound film and the base, the edge extraction accuracy was improved by using coarse positioning first and then fine positioning.

Coarse positioning. Template matching was used for coarse positioning, and the affine transformation matrix was obtained by using the position and angle relationship between the matching region Z'_m and the template region Z_m of the image to be matched, as shown in Fig.10. The affine transformation matrix consisted of two parts: rotation matrix and transfer matrix. The rotation matrix R was obtained according to the angle relationship between the matching region and the template region, the translation matrix T was obtained using the position relationship between them. The final affine transformation matrix H was obtained by multiplying matrix R and T.

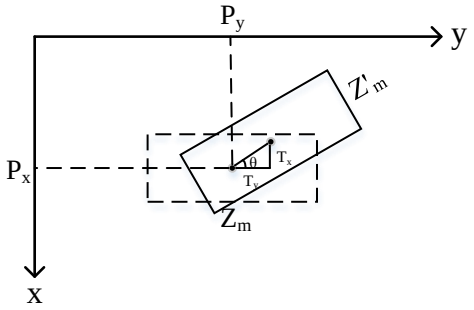

Fig. 10. *Template matching position*

$$H = T \cdot R \tag{7}$$

$$R = \begin{bmatrix} 1 & 0 & P_x \\ 0 & 1 & P_y \\ 0 & 0 & 1 \end{bmatrix} \cdot \begin{bmatrix} \cos\theta & -\sin\theta & 0 \\ \sin\theta & \cos\theta & 0 \\ 0 & 0 & 1 \end{bmatrix} \cdot \begin{bmatrix} 1 & 0 & -P_x \\ 0 & 1 & -P_y \\ 0 & 0 & 1 \end{bmatrix} \tag{8}$$

$$T = \begin{bmatrix} 1 & 0 & T_x \\ 0 & 1 & T_y \\ 0 & 0 & 1 \end{bmatrix} \tag{9}$$

P_x and P_y represented the row and column coordinates of the template center, respectively, θ represented the angle between the matching region Z'_m of the image to be matched and the template region Z_m. T_x and T_y represented the distance that the template center moved on the x and y axes, respectively.

The point of the template image $P_m(row1, column1)$ with matching corresponding point on the image $P'_m(row1', column1')$satisfied the following relations:

$$\begin{bmatrix} row1' \\ column1' \end{bmatrix} = H \cdot \begin{bmatrix} row1 \\ column1 \end{bmatrix}$$

Fine positioning. As shown in Fig.11, n non-parallel auxiliary lines (subject n=4) were drawn on the template image, the endpoint coordinates of each auxiliary line were recorded, the positioning line of each auxiliary line was obtained by fitting the measuring caliper, and then the center point $M\ (row2, column2)$ of the intersection points of the n positioning lines and their average deflection angle α

$$(\alpha = \sum_{i=1}^{n} \frac{\alpha_i}{n})$$

were obtained, as shown in Fig.12(a). Through affine transformation matrix H, the position of the endpoint of the auxiliary line in the image to be measured was obtained, and the auxiliary line was generated, the positioning line was generated by fitting the measuring caliper. The center point N(row2', column2') of the lines' intersection point was located, and the average deflection angle was denoted as

$$\theta(\beta = \sum_{i=1}^{n} \frac{\beta_i}{n}),$$

as shown in Fig.12(b). According to the coordinates of M and N, the angle α and β, the fine positioning affine transformation matrix H_1 was obtained by equation (7)-(9).

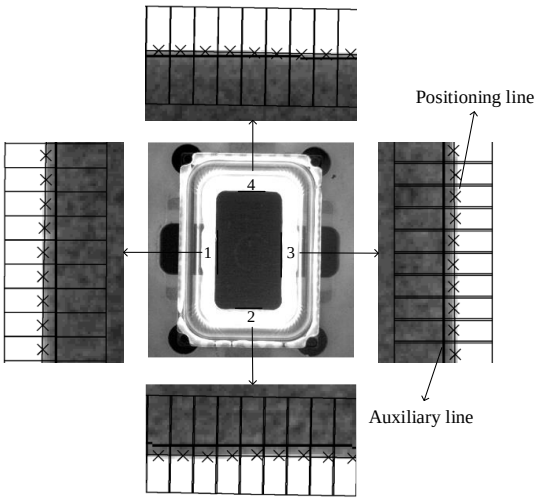

Fig. 11. *Auxiliary line of fine positioning*

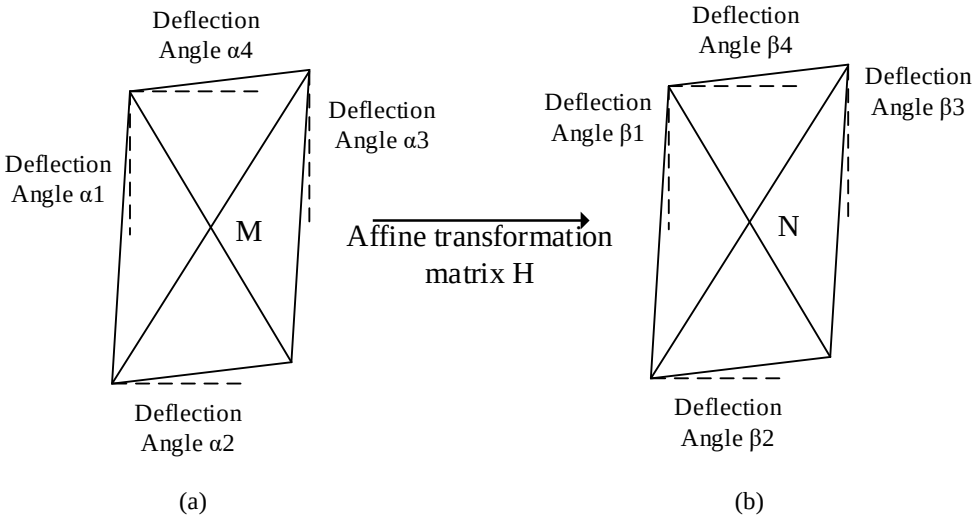

Fig. 12. *Auxiliary line of fine positioning: (a) Template image, (b) Image to be tested*

After the precision positioning, the auxiliary lines of the product edge were drawn on the template image, and the auxiliary lines' positioning line (edge line) was found by measuring the caliper. The intersection coordinates of n edges were obtained, namely n vertices of the product, and the product edges of the template image were generated, as shown in Fig.13(a). The affine transformation matrix H_1 was used to obtain n vertices of the product under the image under test, and then the product edges of the image to be tested were brought.

Identification Of Broken Glue Defects

In order to avoid the influence of the gray level of the sound film background, the image is cropped with the edges of the product as the boundary to obtain a single product image, as shown in Fig.13.

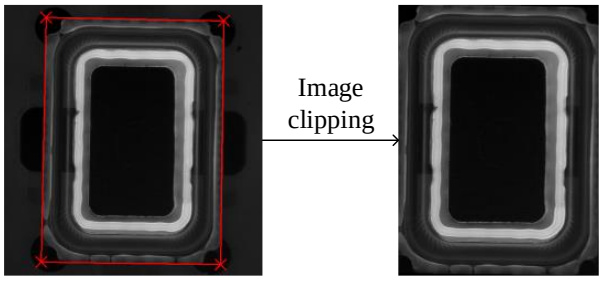

Fig. 13. *Image clipping: (a) Pre-crop image, (b) Image clipping*

After obtaining the glue area by the IIMIV method, the opening operation was used to split the area and calculate the number of glue areas. If the number were greater than 1, it would be judged as a multi-gap defect, as shown in Table 2, the number was 13. If the quantity was equal to 1, for the qualified product, the glue area formed a closed pattern with internal holes, that was, the diagonal part in the figure, for a single gap defect, the glue area cannot form a closed pattern, and there were no holes inside, so qualified products or single-notch defects can be judged by calculating whether the hole area in the glue area was 0.

Table2. *Sound film dispensing quality detection*

Detection result	multi gap defect	qualified product	Single gap defect
Original image			
Threshold segmentation			
Open operation			
Dispersed region			

For the misalignment defect, the product edge was obtained according to the affine transformation matrix H_1, the center coordinate $O_1(r_1,c_1)$ was calculated, then the center coordinate $O_2(r_2,c_2)$ of the glue region was obtained. The Euclidean distance d between O_1 and O_2 was calculated. The misalignment judgment method was as follows:

$$\begin{cases} d = \sqrt{(r_1 - r_2)^2 + (c_1 - c_2)^2} \le D, & \textit{Nonmalposition} \\ d = \sqrt{(r_1 - r_2)^2 + (c_1 - c_2)^2} > D, & \textit{Malposition} \end{cases}$$

D was half of the width of the dispensing area of the product, after obtaining the glue area of the qualified product, filled the area, calculated the height of the area as *h1*, and then made a difference between the filled area and the original glue area to obtain the difference area, calculated the height of the area as *h2*. The difference between *h1* and *h2* was *1/4 D*. As shown in Fig.14.

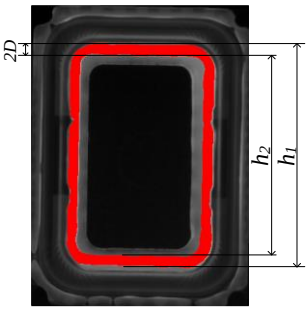

Fig. 14. *Misalignment diagram*

RESULTS

DETECTION EXPERIMENT

In order to verify the accuracy of the detection method, 15,000 products were selected from the production line for retesting. After the unqualified products caused by other defects were removed, the retesting results were shown in Table 3. The detection accuracy of qualified products was 100%, and the detection accuracy of three types of broken glue defects was 98%, 100%, and 100%, respectively, indicating that the algorithm in this paper can accurately identify OK products and broken glue NG products, and distinguished the types of broken glue. Through the analysis, the misjudgment of multi-gap defect detection was because part of the product glue path was thin, which led to the deviation of glue region segmentation during the opening operation. In addition, ten replicates of qualified products and defective products were selected for 100 times detection, and the detection results were consistent, which proved that the stability and accuracy of the detection method were good.

Table 3. *Test results of broken glue quality*

Detection result	Quantity/piece	Miscalculation number/piece	Accuracy rate/%
OK	14836	0	100
Multi gap NG	68	1	98
Single gap NG	40	0	100
Misaligned NG	15	0	100

DISCUSSION

In this paper, aiming at the problem of existing dispensing quality detection in enterprises, a visual detection method of sound film dispensing quality was proposed. According to the gray distribution of the image, abnormal data were removed by an improved iterative method, and the initial segmentation threshold of the sound film dispensing image was obtained, which was combined with the OTSU method to obtain the best segmentation threshold and then accurately extracted the dispensing area. This method improved the traditional OTSU method when the image gray curve had a skewed distribution, the segmentation effect was not ideal. The experimental test showed that the scheme could accurately identify the broken glue defect and distinguish the broken glue type, the overall detection accuracy was 99.1%.

ACKNOWLEDGMENTS

The all authors would like to acknowledge funding from Fujian Province Science and Technology Plan Project, University-industry-research Cooperation Project Fund grant numbe 2021H6036.

REFERENCES

Chen SX, Wang T (2020). Vision-based quality inspection method for glue application. Combined machine tool and automatic processing technology 7:138-141.

Guo YM, Wang Y, Meng K, Zhu ZN (2023). Otsu Multi-Threshold Image Segmentation Based on Adaptive Double-Mutation Differential Evolution. Biomimetics (Basel) 8(5):418.

Guo YK, Zhu YC, Liu LP, Huang Q (2022). A review of research on image enhancement methods in the air-frequency domain. Computer Engineering and Applications 58(11):23-32.

He XH, Chen CG, Zhou C, Xie DF, Xie Hw (2020). Dispensing quality inspection method based on machine vision. Combined Machine Tools and Automated Machining Technology 0(11):99-101,106.

Huang P, Zheng Q, Liang C (2020). A review of image segmentation methods . Journal of Wuhan University (Science Edition) 66(06):519-531.

Liao Y (2015). Design and realization of engine block gluing detection module based on machine vision [D]. Chengdu: University of Electronic Science and Technology.

Liang JL, Ye GL, Guo JW, Wu JX (2023). Research on visual inspection system for button battery defects. Mechanical Design and Manufacturing 385(3):225-229.

Li ZC, Cao YP (2022). Leukocyte image segmentation method based on improved iterative thresholding. Optics and Photonics 20(02):84-94.

Ma W, Li W ,Cao P (2019). Ranging Method of Binocular Stereo Vision Based on Random Ferns and NCC Template Matching. IOP Conference Series: Earth and Environmental Science 252(2).

Shen JH, Wu XJ ,Wang XH, Liang GY (2023). Robust shape-based template matching algorithm for target localization under SEM.. Optics express 31(20) :32652-32668.

Yu YS, Su YF, Gao JS (2023). Algorithm for gluing quality detection based on KNN classification. Combined Machine Tools and Automated Machining Technology 07:127-130.

Yu J, Cheng X, Zhao Z (2022). A machine vision method for measurement of drill tool wear. The International Journal of Advanced Manufacturing Technology 118: 3303-3314.

Zhang JG, Ji TT, Xin MX, Zuo CM, Liu J (2021). Edge extraction method in adhesive coating defect detection. Ship Engineering 43(2):128-133.

Zou R, Dai WJ, Bai SH, Wu SL (2024). Edge-preserving light-field image super-resolution via feature affine transformation network. Optics and Lasers in Engineering 172.